Letter

Magnetic levitation as a new probe of non-Newtonian gravity

Dorian W. P. Amaral,[1,*] Tim M. Fuchs,[2] Hendrik Ulbricht,[2] and Christopher D. Tunnell[1]

[1]*Department of Physics and Astronomy, Rice University, MS-315, Houston, Texas 77005, USA*

[2]*School of Physics and Astronomy, University of Southampton, SO17 1BJ, Southampton, United Kingdom*

(Received 2 July 2025; accepted 6 January 2026; published 27 January 2026)

We present the magnetic oscillatory resonator for rare-interaction studies (MORRIS) and propose the first tabletop search for non-Newtonian gravity due to a Yukawa-like fifth force using a magnetically levitated particle. Our experiment comprises a levitated submillimeter magnet in a superconducting trap that is driven by a time-periodic source. Featuring short-, medium-, and long-term stages, MORRIS will admit increasing sensitivities to the force coupling strength α, optimally probing screening lengths of $\lambda \sim 1$ mm. Our short-term setup provides a proof-of-principle study, with our medium- and long-term stages respectively constraining $\alpha \lesssim 10^{-4}$ and $\alpha \lesssim 10^{-5}$, leading over existing bounds. Our projections are readily recastable to concrete models predicting the existence of fifth forces, and our statistical analysis is generally applicable to well-characterized sinusoidal driving forces. By leveraging ultralow dissipation and heavy test masses, MORRIS opens a new window onto tests of small-scale gravity and searches for physics beyond the Standard Model.

DOI: 10.1103/pqrs-bpgj

Introduction. Despite its success at astrophysical scales, the theory of general relativity remains irreconcilable with quantum mechanics, and no theory of quantum gravity has emerged [1,2]. Precision tests of gravity at millimeter scales and below offer a promising window onto its potential quantum nature. Observed deviations from the Newtonian prediction—the nonrelativistic limit of general relativity—would signal a departure from classical gravity and hint at novel physics beyond the Standard Model [3–5]. These could manifest as violations of the inverse-square law (ISL) and shifts in the expected gravitational interaction strength.

Many beyond Standard Model scenarios lead to modifications of gravity at $\mathcal{O}(1\ \mathrm{mm})$ scales [3,6]. For instance, string theory introduces extra spatial dimensions at these scales, with superstring theory predicting the presence of light moduli fields, both of which result in deviations from Newtonian gravity [7–9]. Meanwhile, incorporating additional gauge symmetries into the Standard Model can result in new massive mediators that propagate Yukawa-like fifth forces [10]. Laboratory searches for millimeter-scale Yukawa forces have primarily employed torsion balances and pendula [11–13], with levitated setups utilizing optically suspended microspheres that have pushed sensitivities into the micron regime [14,15]. However, magnetic levitation strategies are yet to be exploited in the search for a generic fifth force [16,17].

Magnetic levitation setups offer ultralow mechanical dissipation with high quality factors ($Q \gtrsim 10^6$) and the ability to suspend millimeter-scale magnets. This makes them excellent force and acceleration sensors [18–22], with sensitivities reaching values as low as $10^{-16}\mathrm{N\,Hz^{-1/2}}$, allowing them to detect purely gravitational interactions [23]. Unlike optical or electrostatic traps, magnetic levitation relies on passive Meissner repulsion to levitate heavy test masses, introducing virtually no active-feedback noise and boosting the signal for forces that couple proportionally to mass. These features make this technology a powerful choice for probing small deviations from Newtonian gravity and the signals predicted by many beyond Standard Model theories.

Despite its promise, magnetic levitation technology is only now being employed in tests of fundamental physics [24,25]. Levitated magnets have recently been shown to be a leading option in the search for ultralight [26–29] and ultraheavy [30] dark matter, as well as for high-frequency gravitational waves [31]. At the interface of quantum theory and gravity, proposals have also been put forward to search for macroscopic superposition states [25] and to test MOND-like modifications of gravity [32,33]. However, unlike MOND, a generic Yukawa-type parametrization makes no assumption on the acceleration scale at which new physics enters, providing a continuous framework for uncovering deviations from Newtonian gravity across all scales.

In this Letter, we introduce the magnetic oscillatory resonator for rare-interaction studies (MORRIS) and evaluate the sensitivity of the state-of-the-art and beyond in magnetic levitation to non-Newtonian gravity due to an

*Contact author: damaral@ifae.es

additional Yukawa potential. Our proposal employs a submillimeter magnetic particle trapped via the Meissner effect and driven by a time-periodic source. We develop three experimental stages (short-, medium-, and long-term configurations) and use a likelihood-based approach to project our sensitivities to the coupling strength α over screening length λ. By comparing our projections to existing fifth force searches, we demonstrate that MORRIS will be able to uniquely test small-scale gravity and provide broad access to physics beyond the Standard Model.

Fifth forces. A Yukawa potential can be generically parametrized by a dimensionless strength parameter α and a screening length λ. The strength parameter can be positive or negative, leading to either an attractive or a repulsive interaction. Including gravity, the relevant potential for our experiment is

$$U(r) \equiv -\frac{G_\infty m_s m_p}{r}(1 + \alpha e^{-r/\lambda}), \quad (1)$$

where m_s and m_p are the masses of the source and levitated particle, respectively, which are placed a relative distance r away from each other. The constant G_∞ is Newton's gravitational constant.

From this potential, we may compute the total force using $\boldsymbol{F}(\boldsymbol{r}) = -\boldsymbol{\nabla} U(r)$

$$\boldsymbol{F}(\boldsymbol{r}) = -\frac{G_\infty m_s m_p}{r^2}\left[1 + \alpha\left(1 + \frac{r}{\lambda}\right)e^{-r/\lambda}\right]\hat{\boldsymbol{r}}. \quad (2)$$

In our experiment, we generate this force via a time-periodic source. We achieve this by using either a spinning disk with three cylindrical masses removed in the case of our short- and medium-term setups, or a driven magnetically levitated particle within a second trap for our long-term stage. We illustrate these setups in Fig. 1. We place the source at a variable central displacement from the levitated particle r_0, representing the distance between the particle and the midpoint of the oscillation, possessing amplitude R. The most relevant physical scale is the closest approach distance between a source mass and the particle, $a(r_0) \equiv r_0 - R$. By varying this, we obtain sensitivity to ISL violations.

At each central position r_0, we record the motion of the particle along a fixed sensitivity axis $\boldsymbol{\zeta}$ using a superconducting pickup coil coupled to a SQUID. The time-dependent total force is then

$$F_{\text{tot}}(t, r_0) \equiv \sum_{i=1}^{N_{\text{mass}}} \boldsymbol{F}(\boldsymbol{r}_i(t, r_0)) \cdot \hat{\boldsymbol{\zeta}}, \quad (3)$$

where the sum runs over the number of source masses N_{mass}. We align $\boldsymbol{\zeta}$ with the x-axis of our experiment, along which we also place the oscillating source.

To simplify our analysis, we decompose the total force into the sum of a constant component, which is irrelevant for our study, and an oscillatory component, $F_{\text{osc}}(t, r_0) \equiv \mathcal{F}_{\text{osc}}(r_0)\sin(\omega_s t)$. The angular frequency $\omega_s = N_{\text{mass}}\omega_d$ is that of our periodic source, with ω_d the angular frequency of the drive. The amplitude $\mathcal{F}_{\text{osc}}(r_0)$ is given by half the difference between the maximal and minimal driving forces. We visualize the driving force in Fig. 1 and validate our approximation in Ref. [34].

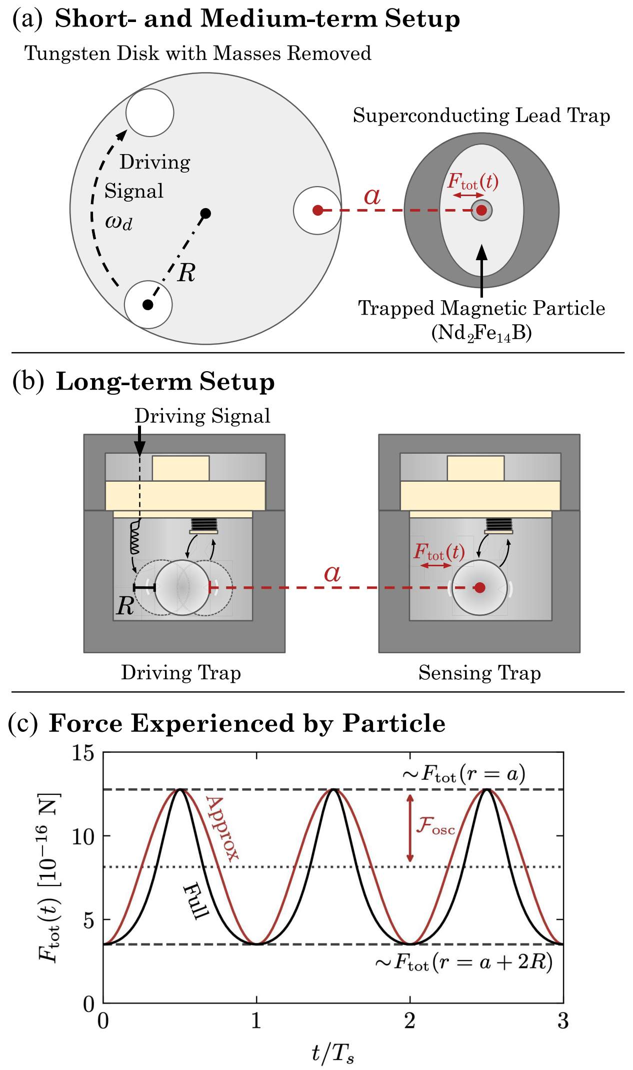

FIG. 1. (a) Top view of the proposed short- and medium-term experimental setups for MORRIS, showing the mass-wheel and the trapped particle. We include the separation between the driving and test masses at closest approach a, the distance modulation R, the frequency of the drive ω_d, and the total force experienced by the particle $F_{\text{tot}}(t)$. (b) Side view of the proposed long-term setup, consisting of two traps. In the driving trap, an AC electromagnetic drive excites the trapped particle. (c) The force experienced by the sensing particle with signal period T_s. The dependence of this force to a and R is explained in Ref. [34].

Ultimately, we conduct our analysis in Fourier space by analyzing the force power spectral density (PSD), $\mathcal{P}(\omega)$. Our signal manifests as a monochromatic peak at the angular frequency ω_s, with a peak height proportional to

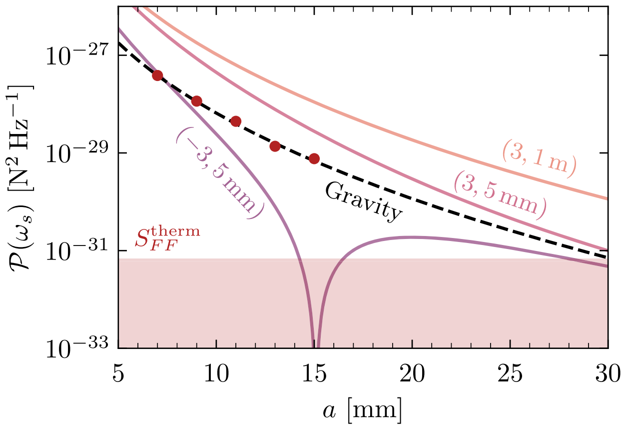

FIG. 2. The force power spectral density of our levitated particle taken at the resonance frequency of the particle, $\mathcal{P}(\omega_s)$, with varying closest approach distance a. We assume our short-term configuration (cf., Table I). Shown is the expected gravitational signal ($\alpha = 0$) with five equally spaced data points (red markers). The fifth-force signals from three benchmark points are also shown, labeled according to (α, λ). The noise floor is assumed to be thermal, $S_{FF}^{noise}(\omega_s) = S_{FF}^{therm}$ [cf., Eq. (5)].

$\mathcal{F}_{osc}^2(r_0)$ [34]. The quantity of interest for our inferencing is the *excess power* at this frequency normalized by the noise PSD $S_{FF}^{noise}(\omega_s)$. The normalized excess power at the central displacement r_0 after observing for a time T_{obs} is given by the square of the quantity

$$\kappa(r_0) \equiv \sqrt{\frac{\mathcal{F}_{osc}^2(r_0) T_{obs}}{2 S_{FF}^{noise}(\omega_s)}}. \tag{4}$$

We show the excess power, $\kappa^2(r_0) S_{FF}^{noise}(\omega_s)$, with varying closest approach distance in Fig. 2 for a choice of benchmark points (α, λ). We assume our short-term configuration, summarized in Table I. We illustrate the gravitational signal ($\alpha = 0$), together with a set of simulated data points. We show the signals from a Yukawa force with parameters (3, 1 m), (3, 5 mm), and (−3, 5 mm). While these benchmark points are already firmly excluded, we visualize them to clearly illustrate the effect of a fifth force in our experiment. Moreover, though we display the signals over the full experimental range, we opt to measure them over a shorter scale to improve our overall signal-to-noise ratio. The noise is assumed to be thermal, $S_{FF}^{noise}(\omega_s) = S_{FF}^{therm}$, as given in Eq. (5) and justified below.

For the first benchmark point, the fifth force is not effectively screened, resulting in a signal that does not observably violate the ISL; it instead appears as a scaling of the gravitational signal. For the remaining benchmark points, ISL violations are expected, with the latter featuring a repulsive force that can lead to a cancellation of the gravitational signal. This can be seen at $a \approx 15$ mm. Since systematic uncertainties can scale our signal but are unlikely to mimic the spectral features induced by ISL violations, we are most sensitive to screening lengths of the order of our shortest experimental scale, $\lambda \sim a_{min} \sim \mathcal{O}(1\ \text{mm} - 10\ \text{mm})$.

TABLE I. The short-, medium-, and long-term configurations for our experiment, MORRIS. Shown is the mass of the levitated particle (m_p), the mass of a single source mass (m_s), the minimum central displacement (r_0^{min}), the minimum closest approach distance (a_{min}), the motional amplitude (R), the observation time for a single data point (T_{obs}), the cooling temperature (T), the resonance frequency of the particle (f_0), the number of driving masses (N_{mass}), the quality factor (Q), and the uncertainty in the pull parameter (σ_ξ).

MORRIS	Short	Medium	Long
m_p [mg]	4	40	400
m_s [mg]	210	350	400
r_0^{min} [mm]	19.5	19.5	3
a_{min} [mm]	7	7	2
R [mm]	12.5	12.5	1
T_{obs} [h]	20	1000	1000
T [K]	4	1	0.1
f_0 [Hz]	35	35	150
N_{mass}	3	3	1
Q	10^6	10^7	10^7
σ_ξ	10%	1%	0.1%

Experiment. We present our proposed experiment, MORRIS, in Fig. 1. At its core is a composite particle consisting of a magnetic core and a nonmagnetic weight that is levitated within a superconducting trap and driven by an external periodic force. We will use $Nd_2Fe_{14}B$ magnets due to their high remnant magnetization to aid in signal detection, silica to add mass without increasing eddy-current damping, and lead traps for their high type-I transition temperature (7.2 K). The magnetic trapping mechanism yields high quality factors Q (in excess of 10^7) at low resonance frequencies f_0 (∼10 Hz) [37]. Low-frequency operation enables the generation of a time-varying force gradient with a high modulation depth, leading to an increased signal. The gradient is sourced near the resonance frequency of the trapped particle, such that its motional amplitude steadily increases. This will be recorded via a pickup coil coupled to a SQUID—the conversion from SQUID signal to motion will be made either through thermal noise calibration or by injecting an external flux signal [23].

Our experiment features short-, medium-, and long-term stages that will allow us to search for non-Newtonian gravity with increasing sensitivities. They are expected to take one, two, and five years to construct, respectively. We summarize them in Table I, providing technical details in Ref. [34].

In the short- and medium-term setups, the force is sourced by a high-density solid disk of radius 1.25 cm with three cylindrical masses removed. This density modulation sources a gradient when the disk is spun, such that the driving force varies with a frequency matching the resonance frequency of our particle. We will use tungsten for its high density, ease of machining, and commercial availability. Unlike in previous work, we will place the driving wheel inside of the cryogenic cooling system to minimize the shortest approach distance and attain sensitivities down to $\lambda \sim 1$ mm [23].

Our proposed long-term realization instead utilizes a direct drive of a particle suspended within a second trap. The second particle is driven either through an electrostatic interaction or via magnetic coils. This setup is similar to that proposed for precision measurements of the gravitational constant and in earlier work performed by the group [32,38]. The geometry of this configuration allows us to achieve a smaller closest approach distance, halving $a_{\min}$, while still guaranteeing adequate shielding from external electromagnetic forces. To minimize this distance, we will reduce the size of the traps from ∼1 cm down to 2.5 mm along the minor axis [23].

During the experiment, sufficiently shielding the particle from external disturbances is crucial. This includes electromagnetic shielding and vibration isolation. Such shielding has been shown to adequately isolate a 0.4 mg mass to a translational mode temperature of below 4 K [23], placing the excess noise below the thermal noise for our short-term stage. Higher levels of vibration isolation have been reported by the LIGO collaboration and implementing similar levels of isolation would allow for thermally limited operation down to 100 mK [39]. Moreover, we will optimize the coupling to the particle's motion such that the SQUID-readout noise is below the thermal noise floor, achieving this by increasing the number of pick-up coil windings and the geometrical coupling to the particles motion. Fiducializing to our short-term setup and using $\gamma \equiv \omega_0/Q$ as our mechanical dissipation rate, our expected thermal noise is

$$S_{FF}^{\text{therm}} = 4 m_p k_B T \gamma \approx 10^{-31}\,\mathrm{N^2 Hz^{-1}} \left(\frac{m_p}{4\ \mathrm{mg}}\right)\left(\frac{T}{4\ \mathrm{K}}\right)\left(\frac{f_0}{35\ \mathrm{Hz}}\right)\left(\frac{10^6}{Q}\right). \tag{5}$$

Systematic uncertainties in our experiment can arise from how precisely we are able to measure masses, displacements, temperatures, and frequencies. In our statistical analysis, we account for them by introducing a pull parameter ξ in our inferencing pipeline. This parameter serves to scale the signal-to-noise ratio and can be interpreted as its fractional uncertainty. A justification for the pull parameter uncertainties is given in Ref. [34].

A key advantage of our experimental strategy is that we have excellent control over our source. Not only can we generate a driving force at a well-characterized frequency, such that we can target the signal in Fourier space, but we can also instrument the source masses to have precisely known values and vary the separation between the source and test particle. Placing the source in the vacuum greatly reduces the minimum separation between the test and source masses, giving us sensitivity to smaller screening lengths λ.

Furthermore, measuring the force at varying separations gives us sensitivity to ISL violations. We will therefore make five equally spaced measurements, beginning from the minimum allowed central displacement of each setup $r_0^{\min}$: 19.5 mm for our short- and medium-term stages and 3 mm for our long-term goal. We will displace the source 2 mm at a time in the first two setups, improving this to 1 mm in the long term. Remaining close to the minimal displacements gives us larger signal-to-noise ratios. Five data points are sufficient to give us competitive sensitivities when spectral information is available while maintaining a realistic total expedition time of $\sim 5T_{\mathrm{obs}}$. From an experimental perspective, sampling at different separations allows for the rejection of systematic errors in both the closest separation a and the force modulation depth by matching the curvature of the results.

Analysis and results. Our expected signal is a monochromatic peak in the force PSD [34]. The likelihood function governing the noise-normalized excess power is a noncentral χ^2 function, χ^2_{nc}, with $k = 2$ degrees of freedom [40]. For the ith data point p_i, taken at the central displacement $r_{0,i}$, the noncentrality parameter is $\kappa_i^2 \equiv \kappa^2(r_{0,i})$. To account for potential systematic uncertainties in both the signal and the noise, we include a nuisance pull parameter ξ in our analysis that we ultimately profile out. This enters as a scaling of the noncentrality parameter, such that $\kappa_i \to (1+\xi)\kappa_i$. We take $\xi \sim \mathcal{N}(0, \sigma_\xi^2)$, where σ_ξ is its uncertainty.

Since each data point is identically and independently distributed, the total likelihood is the product of the likelihood of each individual data point. Including the penalty term for the pull parameter, our likelihood given the observed data vector $\boldsymbol{p} \equiv \{p_i\}$ is

$$\mathcal{L}(\alpha, \lambda, \xi; \boldsymbol{p}) \equiv \prod_{i=1}^{N_{\mathrm{data}}} \chi^2_{\mathrm{nc}}(p_i; (1+\xi)^2 \kappa_i^2, k = 2) \times \frac{1}{\sqrt{2\pi}\sigma_\xi} \exp\left(-\frac{\xi^2}{2\sigma_\xi^2}\right), \tag{6}$$

where $N_{\mathrm{data}} = 5$ is the number of measurements. Using this likelihood, we define the profile likelihood ratio $\lambda_{\mathrm{PLR}}(\alpha, \lambda = \lambda_0; \boldsymbol{p})$, which profiles away the pull parameter. We then construct the two-sided test statistic $t_\alpha \equiv -2\ln[\lambda_{\mathrm{PLR}}(\alpha, \lambda = \lambda_0; \boldsymbol{p})]$ and use it to draw our projected sensitivities [41]. We detail our inference pipeline in Ref. [34], which is generally applicable to searches for well-characterized sinusoidal driving forces.

To calculate our projections, we simulate 10^3 pseudodatasets according to a gravity-only signal. For each $\lambda = \lambda_0$, we scan over α to find our limit, which occurs

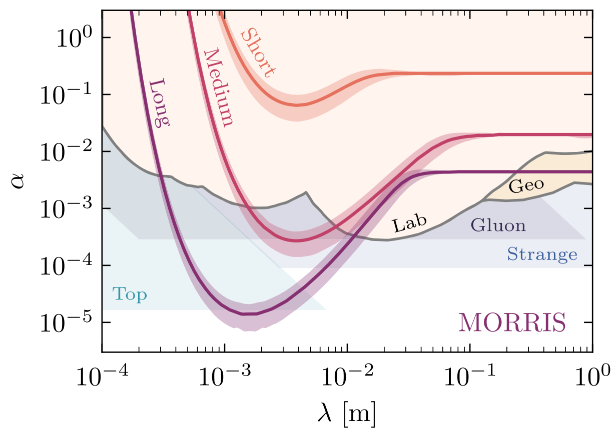

FIG. 3. The 95% confidence level projected limits on positive values of α with scale λ from MORRIS. Shown are the limits from our short-, medium-, and long-term configurations, summarized in Table I. The bands around each limit illustrate their 1σ range. The solid regions indicate the existing fifth-force limits from laboratory [12,13,42,43] and geophysical [3] experiments. The transparent regions show the preferred regions for light moduli arising from supersymmetric string theory [8,9].

when $t_\alpha \approx 3.84$ at the 95% confidence level (CL) [34]. This procedure gives us a distribution of limits, the median of which we take as our best estimator of the limit. We also use these distributions to define 1σ limit bands. Since our projections for positive and negative α are similar, we only visualize our positive sensitivities, providing the full limit landscape in Ref. [34].

We show our projected 95% CL limits in Fig. 3. All limits exhibit the same characteristic behaviors with varying screening length λ. We achieve optimal sensitivity when $\lambda \sim a_{\min}$, the minimum closest approach distance of a source mass. This is because the amplitude $\mathcal{F}_{\rm osc}$ is highly separation dependent, giving the data point at the closest separation the largest signal-to-noise ratio. This leads to a turnover at $\lambda \sim 7$ mm for the short- and medium-term realizations and at $\lambda \sim 2$ mm for the long-term stage (a similar scale to this was found in Ref. [32]). Since our projections are based on a generic Yukawa parametrization, they can be readily recast to concrete models predicting the existence of fifth forces, such as novel light scalar or vector mediators [3].

Below these characteristic distances, the fifth force is effectively screened over the scale of our experiment, leading to an exponential suppression of the signal. Conversely, above these distances, the signal is well described by a scaling of the null gravitational signal, allowing the pull parameter ξ to account for the observed effect. At these high λ values, the limiting α is dictated by the uncertainty in the pull parameter σ_ξ, such that $\alpha \sim \sigma_\xi$. Analytical estimates of our sensitivities, which corroborate with our numerical results, are given in Ref. [34].

We compare our projections to existing laboratory and geophysical constraints in the λ range of interest. The former consists of torsion balance [12,42] and pendulum [13,43] experiments, while the latter includes precision measurements of Earth's gravitational acceleration [3]. Our short-term sensitivity, which is based on an immediately realizable configuration, provides a proof-of-concept for our experiment. Following a set of simple upgrades, a medium-term experiment will have leading sensitivity and constrain $\alpha \lesssim 10^{-4}$ at a screening length of $\lambda \approx 4$ mm. Our long-term experiment is sensitive to new parameter space over the screening length range 0.3 mm to 10 mm, constraining $\alpha \lesssim 10^{-5}$ at $\lambda \approx 2$ mm and surpassing laboratory limits by two orders of magnitude.

The final two stages of our experiment will test regions of parameter space preferred by supersymmetric string theory [8,9]. Superstring theory introduces light moduli fields with masses governed by the supersymmetry breaking scale $\mathcal{F}_s$. These new scalar fields can mediate Yukawa-like fifth forces that couple to ordinary matter, as is the case for Yukawa and gauge moduli. The impact of these moduli in the fifth-force landscape is typically visualized in the submillimeter regime by assuming a cutoff scale of $\mathcal{F}_s \sim (10\ \text{TeV})^2$; however, a higher scale of $\mathcal{F}_s \sim (2000\ \text{TeV})^2$ is also well motivated [9,44]. This extends the moduli regions to millimeter scales, where our experiment is highly sensitive. We show the preferred regions for the gluon, strange quark, and top quark moduli.

Conclusions. We have introduced MORRIS and evaluated the sensitivity of magnetic levitation technology to non-Newtonian gravity. Our proposed tabletop experiment features a periodic source effecting a driving force on a levitated permanent magnet inside a superconducting trap. We considered a general Yukawa-like fifth force, described by a coupling strength α and screening length λ, that induces violations of the inverse-square law. We developed a likelihood framework generally applicable to searches for well-characterized sinusoidal driving forces, using it to compute the projected sensitivities of short-, medium-, and long-term realizations of our experiment. Our medium- and long-term stages will achieve leading sensitivities at millimeter scales in λ ($\alpha \lesssim 10^{-4}$ and $\alpha \lesssim 10^{-5}$, respectively), with the latter boasting two orders of magnitude greater sensitivity than existing limits. These results can be readily recast to concrete models predicting the existence of fifth forces. Our work demonstrates the promise of magnetic levitation in gravity tests at the quantum frontier and in broader searches for physics beyond the Standard Model.

Acknowledgments. We thank Mustafa Amin, Andrew Long, Louis Hamaide, and Juehang Qin for their valuable comments on the manuscript. D. A. thanks Juehang Qin for helpful discussions on our statistical analysis, as well as Mustafa Amin and Andrew Long for insightful discussions throughout this work. D. A. and C. T. were jointly funded by Rice University and NSF award 2046549. T. F. and H. U. were supported by the EU Horizon Europe EIC

Pathfinder project QuCoM (10032223) and as part of the EU QUANT-ERA project LEMAQUME, as well as by the UK funding agencies EPSRC (Grants No. EP/V000624/1, No. EP/V035975/1, No. EP/W007444/1, No. EP/X009491/1) and STFC via the Southampton IAA project DMLOMS, by the Leverhulme Trust (RPG-2022-57), by ESA as parts of the Payload masters competition and by UKSA as part of the IBF project I3F.

Data availability. The data supporting this study's findings are available within the article.

[1] R. Penrose, On the gravitization of quantum mechanics 1: Quantum state reduction, Found. Phys. **44**, 557 (2014).

[2] D. M. Greenberger, The disconnect between quantum mechanics and gravity, in *Quantum Physics and the Nature of Reality: A Conference in Honour of John Polkinghorne's 80th Birthday* (2010), arXiv:1011.3719.

[3] E. G. Adelberger, B. R. Heckel, and A. E. Nelson, Tests of the gravitational inverse square law, Annu. Rev. Nucl. Part. Sci. **53**, 77 (2003).

[4] C. M. Will, The confrontation between general relativity and experiment, Living Rev. Relativity **9**, 3 (2006).

[5] S. Hossenfelder, Experimental search for quantum gravity, in *Classical Quantum Gravity: Theory, Analysis and Applications* (2010), arXiv:1010.3420.

[6] E. G. Adelberger, J. H. Gundlach, B. R. Heckel, S. Hoedl, and S. Schlamminger, Torsion balance experiments: A low-energy frontier of particle physics, Prog. Part. Nucl. Phys. **62**, 102 (2009).

[7] N. Arkani-Hamed, S. Dimopoulos, and G. R. Dvali, The hierarchy problem and new dimensions at a millimeter, Phys. Lett. B **429**, 263 (1998).

[8] S. Dimopoulos and G. F. Giudice, Macroscopic forces from supersymmetry, Phys. Lett. B **379**, 105 (1996).

[9] S. Dimopoulos and A. A. Geraci, Probing submicron forces by interferometry of Bose-Einstein condensed atoms, Phys. Rev. D **68**, 124021 (2003).

[10] E. Fischbach and C. Talmadge, Six years of the fifth force, Nature (London) **356**, 207 (1992).

[11] A. A. Geraci, S. B. Papp, and J. Kitching, Short-range force detection using optically-cooled levitated microspheres, Phys. Rev. Lett. **105**, 101101 (2010).

[12] D. J. Kapner, T. S. Cook, E. G. Adelberger, J. H. Gundlach, B. R. Heckel, C. D. Hoyle, and H. E. Swanson, Tests of the gravitational inverse-square law below the dark-energy length scale, Phys. Rev. Lett. **98**, 021101 (2007).

[13] S.-Q. Yang, B.-F. Zhan, Q.-L. Wang, C.-G. Shao, L.-C. Tu, W.-H. Tan, and J. Luo, Test of the gravitational inverse square law at millimeter ranges, Phys. Rev. Lett. **108**, 081101 (2012).

[14] C. P. Blakemore, A. Fieguth, A. Kawasaki, N. Priel, D. Martin, A. D. Rider, Q. Wang, and G. Gratta, Search for non-Newtonian interactions at micrometer scale with a levitated test mass, Phys. Rev. D **104**, L061101 (2021).

[15] G. Venugopalan *et al.*, Search for new interactions at the micron scale with a vector force sensor, arXiv:2412.13167.

[16] J. Prat-Camps, C. Teo, C. C. Rusconi, W. Wieczorek, and O. Romero-Isart, Ultrasensitive inertial and force sensors with diamagnetically levitated magnets, Phys. Rev. Appl. **8**, 034002 (2017).

[17] M. Janse, D. G. Uitenbroek, L. van Everdingen, J. Plugge, B. Hensen, and T. H. Oosterkamp, Current experimental upper bounds on spacetime diffusion, Phys. Rev. Res. **6**, 033076 (2024).

[18] A. Vinante, P. Falferi, G. Gasbarri, A. Setter, C. Timberlake, and H. Ulbricht, Ultralow mechanical damping with Meissner-levitated ferromagnetic microparticles, Phys. Rev. Appl. **13**, 064027 (2020).

[19] C. Gonzalez-Ballestero, M. Aspelmeyer, L. Novotny, R. Quidant, and O. Romero-Isart, Levitodynamics: Levitation and control of microscopic objects in vacuum, Science **374**, eabg3027 (2021).

[20] M. Gutierrez Latorre, G. Higgins, A. Paradkar, T. Bauch, and W. Wieczorek, Superconducting microsphere magnetically levitated in an anharmonic potential with integrated magnetic readout, Phys. Rev. Appl. **19**, 054047 (2023).

[21] J. Hofer, R. Gross, G. Higgins, H. Huebl, O. F. Kieler, R. Kleiner, D. Koelle, P. Schmidt, J. A. Slater, M. Trupke, K. Uhl, T. Weimann, W. Wieczorek, and M. Aspelmeyer, High-*q* magnetic levitation and control of superconducting microspheres at millikelvin temperatures, Phys. Rev. Lett. **131**, 043603 (2023).

[22] P. Schmidt *et al.*, Remote sensing of a levitated superconductor with a flux-tunable microwave cavity, Phys. Rev. Appl. **22**, 014078 (2024).

[23] T. M. Fuchs, D. G. Uitenbroek, J. Plugge, N. van Halteren, J.-P. van Soest, A. Vinante, H. Ulbricht, and T. H. Oosterkamp, Measuring gravity with milligram levitated masses, Sci. Adv. **10**, eadk2949 (2024).

[24] A. Vinante, C. Timberlake, and H. Ulbricht, Levitated micromagnets in superconducting traps: A new platform for tabletop fundamental physics experiments, Entropy **24**, 1642 (2022).

[25] S. Bose, I. Fuentes, A. A. Geraci, S. M. Khan, S. Qvarfort, M. Rademacher, M. Rashid, M. Toroš, H. Ulbricht, and C. C. Wanjura, Massive quantum systems as interfaces of quantum mechanics and gravity, Rev. Mod. Phys. **97**, 015003 (2025).

[26] G. Higgins, S. Kalia, and Z. Liu, Maglev for dark matter: Dark-photon and axion dark matter sensing with levitated superconductors, Phys. Rev. D **109**, 055024 (2024).

[27] R. Li, S. Lin, L. Zhang, C. Duan, P. Huang, and J. Du, Search for ultralight dark matter with a frequency adjustable diamagnetic levitated sensor, Chin. Phys. Lett. **40**, 069502 (2023).

[28] E. Kilian *et al.*, Dark matter searches with levitated sensors, AVS Quantum Sci. **6**, 030503 (2024).
[29] D. W. P. Amaral, D. G. Uitenbroek, T. H. Oosterkamp, and C. D. Tunnell, First search for ultralight dark matter using a magnetically levitated particle, Phys. Rev. Lett. **134**, 251001 (2025).
[30] J. Qin *et al.*, Mechanical sensors for ultraheavy dark matter searches via long-range forces, Phys. Rev. D **112**, 072003 (2025).
[31] D. Carney, G. Higgins, G. Marocco, and M. Wentzel, Superconducting levitated detector of gravitational waves, Phys. Rev. Lett. **134**, 181402 (2025).
[32] C. Timberlake, A. Vinante, F. Shankar, A. Lapi, and H. Ulbricht, Probing modified gravity with magnetically levitated resonators, Phys. Rev. D **104**, L101101 (2021).
[33] M. Milgrom, A modification of the Newtonian dynamics as a possible alternative to the hidden mass hypothesis, Astrophys. J. **270**, 365 (1983).
[34] See Supplemental Material at http://link.aps.org/supplemental/10.1103/pqrs-bpgj, which also includes Refs. [35,36], for further details on our fifth force signal approximation, employed statistics, full limit landscape, analytical sensitivity estimates, and technical details of our experimental choices.
[35] D. Baxter *et al.*, Recommended conventions for reporting results from direct dark matter searches, Eur. Phys. J. C **81**, 907 (2021).
[36] L. Dania, D. S. Bykov, F. Goschin, M. Teller, A. Kassid, and T. E. Northup, Ultrahigh quality factor of a levitated nanomechanical oscillator, Phys. Rev. Lett. **132**, 133602 (2024).
[37] A. Vinante, P. Falferi, G. Gasbarri, A. Setter, C. Timberlake, and H. Ulbricht, Ultralow mechanical damping with meissner-levitated ferromagnetic microparticles, Phys. Rev. Appl. **13**, 064027 (2020).
[38] F. J. Headley, A. Belenchia, M. Paternostro, and D. Braun, Quantum metrology of Newton's constant with levitated mechanical systems, arXiv:2503.16215.
[39] F. Matichard *et al.*, Seismic isolation of advanced LIGO: Review of strategy, instrumentation and performance, Classical Quantum Gravity **32**, 185003 (2015).
[40] E. J. Groth, Probability distributions related to power spectra. Astrophys. J. Suppl. Ser. **29**, 285 (1975).
[41] G. Cowan, K. Cranmer, E. Gross, and O. Vitells, Asymptotic formulae for likelihood-based tests of new physics, Eur. Phys. J. C **71**, 1554 (2011); Eur. Phys. J. C **73**, 2501(E) (2013).
[42] J. K. Hoskins, R. D. Newman, R. Spero, and J. Schultz, Experimental tests of the gravitational inverse square law for mass separations from 2-cm to 105-cm, Phys. Rev. D **32**, 3084 (1985).
[43] W.-H. Tan *et al.*, Improvement for testing the gravitational inverse-square law at the submillimeter range, Phys. Rev. Lett. **124**, 051301 (2020).
[44] G. F. Giudice and R. Rattazzi, Theories with gauge mediated supersymmetry breaking, Phys. Rep. **322**, 419 (1999).